



Citation for published version:

Littlejohn, S, Nogaret, A, Davies, SR, Henini, M, Beere, HE & Ritchie, DA 2011, 'Microwave power generation by magnetic superlattices', Applied Physics Letters, vol. 99, no. 24, 242107. <https://doi.org/10.1063/1.3670400>

DOI:

[10.1063/1.3670400](https://doi.org/10.1063/1.3670400)

Publication date:

2011

Document Version

Publisher's PDF, also known as Version of record

[Link to publication](#)

Copyright (2011) American Institute of Physics. This article may be downloaded for personal use only. Any other use requires prior permission of the author and the American Institute of Physics.

The following article appeared in Littlejohn, S., Nogaret, A., Davies, S. R., Henini, M., Beere, H. E. and Ritchie, D. A., 2011. Microwave power generation by magnetic superlattices. Applied Physics Letters, 99 (24), 242107 and may be found at <http://apl.aip.org/>

University of Bath

General rights

Copyright and moral rights for the publications made accessible in the public portal are retained by the authors and/or other copyright owners and it is a condition of accessing publications that users recognise and abide by the legal requirements associated with these rights.

Take down policy

If you believe that this document breaches copyright please contact us providing details, and we will remove access to the work immediately and investigate your claim.

Microwave power generation by magnetic superlattices

S. Littlejohn,¹ A. Nogaret,^{1,a)} S. R. Davies,¹ M. Henini,² H. E. Beere,³ and D. A. Ritchie³

¹Department of Physics, University of Bath, Bath BA2 7AY, United Kingdom

²School of Physics and Astronomy, University of Nottingham, Nottingham NG7 2RD, United Kingdom

³Cavendish Laboratory, University of Cambridge, Cambridge CB3 0HE, United Kingdom

(Received 30 September 2011; accepted 28 November 2011; published online 14 December 2011)

We report on microwave power emission by ballistic electrons as they cross a region of spatially inhomogeneous magnetic field. Magnetic finger gates were fabricated at the surface of high mobility GaAs/AlGaAs Hall bars embedded in a coplanar waveguide. By modulating the current injected through the Hall bar and measuring the second harmonic of the signal rectified by a Schottky detector, we obtain the microwave power emitted by the superlattice. This power ($\sim 6 \text{ W m}^{-2}$) is compared to the fluorescence of electron spins that undergo spin resonance as they cross domains of opposite magnetic field. © 2011 American Institute of Physics. [doi:10.1063/1.3670400]

The scaling of integrated circuits has been accompanied by a decrease in pitch and cross-sectional area of interconnects to the point where today, the main limitation to the increase in computer speed is the parasitic resistance, inductance, and capacitance of metal wires. While state of the art metal oxide field effect transistors operate above 100 GHz,¹ metal interconnects exhibit losses of -60 dB/cm to -115 dB/cm at 100 GHz that are severe enough to cripple circuit operation.² To significantly increase system performance, several groups have advocated building wireless inter-/intra-chip interconnects as a substitute for physical wires.^{3,4} To implement this vision, ultra-small microwave sources must be conceived that are compatible with standard processing techniques. Microwave emission on the nanoscale has already been demonstrated in spin valves⁵⁻⁷ and molecular magnets.^{8,9}

Here we demonstrate microwave emission from a two-dimensional electron system modulated by a periodic magnetic field that varies on the scale of the mean free path. The device is embedded in a coplanar waveguide that collects the microwave signal, filters it and, using an integrated Schottky diode, down converts it to a dc voltage. We verify that this voltage is proportional to the second derivative of the Schottky current-voltage (I - V) curve and obtain the microwave power emitted per unit area by fitting the theory to the experimental data. The dependency of the microwave emission on temperature, injection current and the magnetization of the grating is reported. It is found to be consistent with the fluorescence of electron spins that undergo spin resonance as they travel ballistically through domains of opposite magnetic field.^{10,11}

Arrays of cobalt finger gates were fabricated on two types of Hall bars. Sample A incorporated a high mobility 2D hole gas grown on a (311)A GaAs substrate,¹² whereas sample B was a standard high electron mobility transistor heterojunction. The carrier mobilities and densities were $\mu = 112\,000 \text{ cm}^2 \text{ V}^{-1} \text{ s}^{-1}$, $p_s = 1.4 \times 10^{11} \text{ cm}^{-2}$ (A) and $\mu = 925\,700 \text{ cm}^2 \text{ V}^{-1} \text{ s}^{-1}$, $n_s = 1.27 \times 10^{11} \text{ cm}^{-2}$ (B). The cobalt fingers were $0.7 \mu\text{m}$ wide, 380 nm thick and pitched

every $1.5 \mu\text{m}$ over a $240 \mu\text{m} \times 500 \mu\text{m}$ area at the centre of the Hall bar—see Fig. 1(b). We magnetized the grating in the plane and perpendicular to the stripes (B_{\perp}) to modulate the heterojunction with the stray magnetic field of the cobalt stripes and obtain magnetic field domains that alternate in sign. The modulation field profile $B_m(x)$ was calculated using

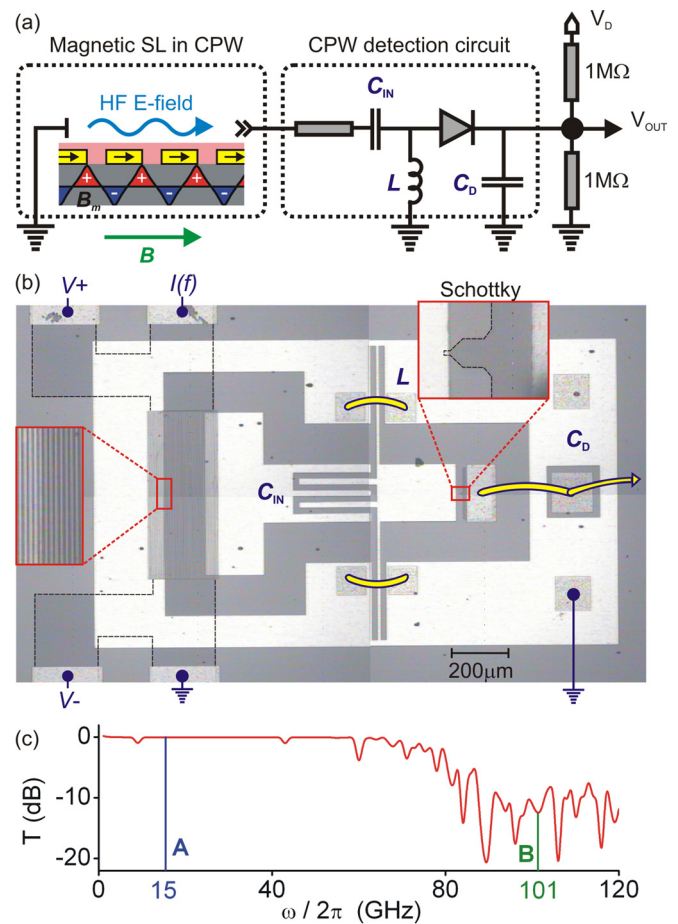


FIG. 1. (Color online) (a) CPW detector circuit and (b) micrograph. Microwave modes propagate from the magnetically modulated Hall bar at the left, through series and shunt filter elements towards the Schottky diode at the right. The stripes are magnetized by magnetic field, B , to modulate the two-dimensional electron/hole gas with the stray field B_m . (c) Transmission spectrum of the CPW structure that includes the filter elements.

^{a)}Author to whom correspondence should be addressed. Electronic mail: A.R.Nogaret@bath.ac.uk, Tel.: +44 (0)1225 385609.

magnetostatics¹³ and plotted in Fig. 1(a). Its amplitude is 0.15 T. The grating was then coated with a SiO₂ film and integrated in a coplanar waveguide (CPW)—see Fig. 1(b). Microwave modes propagate from left to right passing through series (C_{IN} , C_D) and shunt circuit elements (L) before reaching the Schottky diode detector.¹⁴ The Schottky diode was fabricated by etching a $2 \mu\text{m}^2$ tip of two-dimensional hole/electron gas underneath the central strip of the CPW to obtain a low capacitance/wideband detector with excellent rectifying properties—see insets to Figs. 2(c) and 2(d). At microwave frequencies the shunt inductor acts as an open switch while the cathode is effectively grounded. This enables the microwave voltage $v(t) = v_0 \cos(\omega t)$ to be applied in full across the Schottky diode. The Schottky diode down-converts this microwave voltage to a direct current,¹⁵ $I_{DC}(V_D) = \frac{v_0^2}{4} \frac{d^2 I}{dV^2} |_{V_D}$, which is proportional to the microwave power and the second derivative of the Schottky I - V curve at diode bias V_D . We measure the voltage V_{OUT} generated by this current as it passes through the $1 \text{ M}\Omega$ resistors. Note that the shunt inductor drains I_{DC} to the ground, while C_D acts as an open switch enabling V_{OUT} to be measured. The capacitor C_{IN} decouples the source from the detector at low frequency. Fig. 1(c) plots the transmission spectrum of the CPW—including filter elements—calculated using a three-dimensional finite element solver. The bandwidth is 74 GHz while the low attenuation (-0.01 dB) is optimum for measuring low power levels.

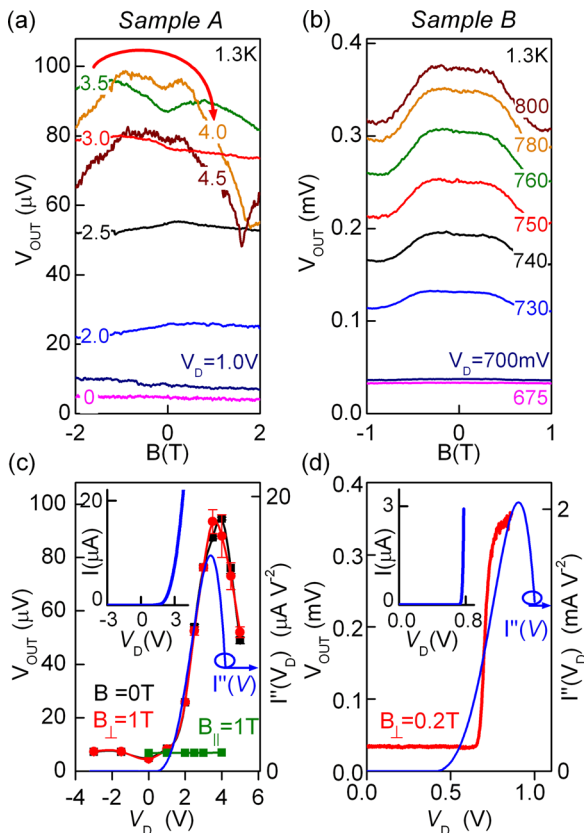


FIG. 2. (Color online) Magnetic field dependence of V_{OUT} in (a) sample A and (b) sample B. $I = 10 \mu\text{A}$ (A), $7 \mu\text{A}$ (B). The curves are parametrized by the Schottky diode bias V_D . (c) and (d) Dependence of V_{OUT} on V_D measured with B in the plane of the heterojunction and perpendicular to the stripes (B_{\perp} dots - red online) or parallel to the stripes (B_{\parallel} squares - green online) compared to the second derivative of the Schottky I - V curves (full lines - blue online).

A current $I(f) = 0$ – $20 \mu\text{A}$ was injected through the magnetic superlattice [Fig. 1(a)]. This current was modulated at a frequency $f = 13 \text{ Hz}$ to enable us to distinguish the down-converted current component from the finite dc current flowing through the diode due to the applied bias V_D . The dc component was filtered out using a lock-in amplifier. We found V_{OUT} to be largest at twice the modulation frequency as expected from the relation $I_{DC} \propto v_0^2(f)$. We then studied the dependency of V_{OUT} on the static bias voltage V_D of the Schottky diode—see Fig. 2. In Figs. 2(c) and 2(d) this dependency (red/green lines) is fitted with the theoretical curve $V_{OUT}(V_D) = (1\text{M}\Omega || 1\text{M}\Omega) \times \frac{v_0^2}{4} \frac{d^2 I}{dV^2} |_{V_D}$ (blue lines) using v_0 as the adjustment parameter. The second derivative $\frac{d^2 I}{dV^2} |_{V_D}$ was obtained by numerically differentiating the Schottky I - V curves which were measured separately—see inset. Figs. 2(c) and 2(d) thus demonstrate the proportionality of the rectified output signal to the second derivative of the I - V curves of the detector. The fit gives $v_0 = 6.7 \pm 0.5 \text{ mV}$ (A) and $v_0 = 1.3 \pm 0.07 \text{ mV}$ (B). The flux of microwave energy radiated perpendicular to the surface of the grating follows as $S = \sqrt{\frac{1+\epsilon_r}{2}} \frac{\epsilon_0 c}{2} \left(\frac{v_0}{d}\right)^2$ where $\epsilon_r = 10.89$ is the relative dielectric constant of GaAs, ϵ_0 is the permittivity of the vacuum, c is the speed of light, and $d = 150 \mu\text{m}$ is the gap between coplanar strips. Using the above values for v_0 , one obtains $S_A = 6.4 \text{ W m}^{-2}$ and $S_B = 0.34 \text{ W m}^{-2}$. In other words, the integral power emanating from each device is 570 nW (A) and 30 nW (B).

When the cobalt stripes are magnetized parallel to their long axis (B_{\parallel}), no magnetic modulation is applied and we observe that V_{OUT} is small and independent of V_D —see Fig. 2(c). We also find that V_{OUT} decreases when the

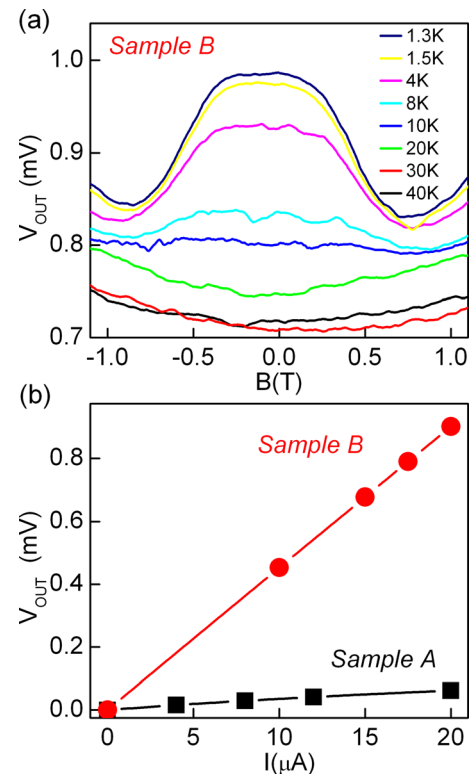


FIG. 3. (Color online) (a) Temperature dependence of V_{OUT} . (b) Dependence of V_{OUT} on the current I injected through the magnetic superlattice ($B = 0 \text{ T}$).

temperature increases from 1.3 K to 20 K. Above 20 K, V_{OUT} has almost vanished. Magnetotransport experiments on device B show that from 1.3 K to 20 K, the electron mean free path drops from 12 μm to 2.3 μm which is only slightly larger than the period of the superlattice. This indicates that microwave emission is dependent on having a magnetic field varying spatially on the scale of the mean free path. Lastly, we measured the dependence of V_{OUT} on the injection current and found the linear dependence shown in Fig. 3(c). This dependence has been predicted for microwave generation via the mechanism of electrically induced spin resonance fluorescence.^{10,11}

Electrically induced spin resonance fluorescence occurs when carriers cross domains of positive and negative magnetic fields such as those realized by placing micromagnets at the surface of a two-dimensional electron system. For ballistic electrons that travel near the Fermi velocity the inhomogeneous magnetic field effectively behaves as a radio frequency (RF) magnetic field. This RF field, combined with the static in-plane magnetic field can induce spin resonance under conditions examined in Refs^{10,11}. Theoretical estimates of the microwave power emitted by magnetic edge states¹¹ give ~ 2 nW for an area 1 mm long and 500 nm wide. This corresponds to an energy flux of ~ 8 W m⁻² which is comparable to the power we obtained experimentally. The theory also provides an explanation as to why the microwave power emitted by the electron gas is lower than that emitted by the hole gas. The spin resonance fluorescence peaks at frequency $f_c = \sqrt{\hbar k_F e b} / (2\pi m^*)$, where $k_F = \sqrt{2\pi n_s}$ is the Fermi wavevector, $b \approx 1$ T/ μm is the magnetic field gradient at the domain boundary, and m^* is the effective mass.¹⁰ The peak frequency being inversely proportional to the effective mass, we find $f_c = 15.4$ GHz for sample A ($m^* = 0.45m_0$) and

$f_c = 101.3$ GHz for sample B ($m^* = 0.067m_0$)—see Fig. 1(c). Peak A is thus well within the 74 GHz bandwidth of the CPW whereas peak B is outside the bandwidth and is attenuated by at least -13 dB. This explains the lower power measured for sample B.

In summary, on-chip power measurements provide evidence of microwave emission by magnetic superlattices. The experimental data are consistent with the mechanism of spin resonance fluorescence.

The authors wish to acknowledge the financial support of the EPSRC (UK) under Grant EP/E002390.

- ¹J. D. Meindl, Q. Chen, and J. A. Davis, *Science* **293**, 2044 (2001).
- ²J. A. Davis, V. K. De, and J. D. Meindl, *IEEE Trans. Electron. Devices* **45**, 590 (1998).
- ³M. C. F. Chang, V. P. Roychowdhury, L. Zhang, H. Shin, and Y. Qian, *Proc. IEEE* **89**, 456 (2001).
- ⁴M. Sun and Y. P. Zhang, *IEEE Trans. Microwave Tech.* **53**, 2650 (2005).
- ⁵S. I. Kiselev, J. C. Sankey, I. N. Krivorotov, N. C. Emley, R. J. Schoelkopf, R. A. Buhrman, and D. C. Ralph, *Nature* **425**, 380 (2003).
- ⁶S. Kaka, M. R. Pufall, W. H. Rippard, T. J. Silva, S. E. Russek, and J. A. Katine, *Nature* **437**, 289 (2005).
- ⁷F. B. Mancoff, N. D. Rizzo, B. N. Engel, and S. Tehrani, *Nature* **437**, 393 (2005).
- ⁸J. Tejada, E. M. Chudnovsky, J. M. Hernandez, and R. Amigo, *Appl. Phys. Lett.* **84**, 2373 (2004).
- ⁹E. M. Chudnovsky and D. A. Garanin, *Phys. Rev. Lett.* **89**, 157201 (2002).
- ¹⁰A. Nogaret and F. M. Peeters, *Phys. Rev. B* **76**, 075311 (2007).
- ¹¹A. Nogaret, N. J. Lambert, and F. M. Peeters, *Phys. Rev. B* **76**, 075312 (2007).
- ¹²M. Henini, P. A. Crump, P. J. Rodgers, B. L. Gallagher, A. J. Vickers, and G. Hill, *J. Cryst. Growth* **150**, 446 (1995).
- ¹³A. Nogaret, *J. Phys. Condens. Matter* **22**, 253201 (2010).
- ¹⁴K. C. Gupta, R. Garg, and I. J. Bahl, *Microstrip Lines and Slotlines* (Artech House, Inc., Massachusetts, 1979).
- ¹⁵D. M. Pozar, *Microwave Engineering*, 2nd ed. (Wiley, New York, 1998).